PHYSICS

Nonequilibrium optical control of dynamical states in superconducting nanowire circuits

Ivan Madan,[1]*† Jože Buh,[1,2]* Vladimir V. Baranov,[3] Viktor V. Kabanov,[1] Aleš Mrzel,[1] Dragan Mihailovic[1,2,4,5]‡

Optical control of states exhibiting macroscopic phase coherence in condensed matter systems opens intriguing possibilities for materials and device engineering, including optically controlled qubits and photoinduced superconductivity. Metastable states, which in bulk materials are often associated with the formation of topological defects, are of more practical interest. Scaling to nanosize leads to reduced dimensionality, fundamentally changing the system's properties. In one-dimensional superconducting nanowires, vortices that are present in three-dimensional systems are replaced by fluctuating topological defects of the phase. These drastically change the dynamical behavior of the superconductor and introduce dynamical periodic long-range ordered states when the current is driven through the wire. We report the control and manipulation of transitions between different dynamically stable states in superconducting δ_3-MoN nanowire circuits by ultrashort laser pulses. Not only can the transitions between different dynamically stable states be precisely controlled by light, but we also discovered new photoinduced hidden states that cannot be reached under near-equilibrium conditions, created while laser photoexcited quasi-particles are outside the equilibrium condition. The observed switching behavior can be understood in terms of dynamical stabilization of various spatiotemporal periodic trajectories of the order parameter in the superconductor nanowire, providing means for the optical control of the superconducting phase with subpicosecond control of timing.

INTRODUCTION

Metastable quantum states are of great importance in areas ranging from fundamental physics to complex materials and many applications (*1*, *2*). Although metastable states are relatively common in condensed matter (*3*–*5*), control of such quantum systems is a big challenge, and there are a very limited number of systems in which these states are long-lived (*6*). A particularly interesting case appears when a new many-body state with long-range order forms only under nonequilibrium conditions. If such a state cannot be reached by a temperature variation or other adiabatic perturbation, then it is commonly called a hidden state.

The most common cause of metastability in condensed matter systems is associated with slow relaxation dynamics of topological defects, such as domain walls created as a result of a rapid thermal quench (*2*, *7*–*9*). In bulk superconductors, photoexcitation usually leads to short-lived states (*10*), whereas the long-lived dynamics is usually associated with topological defects, which in this case are vortex excitations (*11*). This situation is qualitatively different in current-carrying nanoscale superconducting circuits, where the condensate starts to behave as a fundamentally one-dimensional (1D) system. In these circuits, superconducting vortices are replaced by spatially and temporally localized "slips" of phase θ of the superconducting order parameter $\psi = |\psi| e^{i\theta}$ on a scale of the superconducting coherence length ξ at points along the wire (Fig. 1).

This current-driven phase slippage occurs when the Cooper pairs are accelerated to the point where kinetic energy is sufficient for depairing, leading to a collapse of the superfluid density ($n_s \sim |\psi|^2$). The collapse occurs most rapidly if it is localized in the region of the size ξ. Because of depairing, the total current in this region is overtaken by the normal carriers, which leads to the dissipation and appearance of a voltage across the phase slip. The collapse of the condensate introduces discontinuity of the order parameter, hence allowing the variation of the relative phase of the order parameters of two superconducting parts. To restore the continuity of the order parameter, the phase change should be proportional to the factor of 2π. Phase slippage reduces the local phase gradient, which implies the reduction of the supercurrent, and thus allows the healing of the condensate. Because the superfluid density recovers to its initial value, the whole process repeats itself. This unusual state combines superconductivity with dissipation and is intrinsically nonequilibrium.

Similar to the case of the ac Josephson effect, the phase variation across a single phase slip is synchronized with a potential difference; that is, the voltage V_i, giving the frequency of phase slippage, defined as $\nu_J = \frac{2eV}{hn}$. Here, n is the number of phase slips, h is Planck's constant, and $V = \Sigma V_i$ is the total voltage across the wire (*12*, *13*). Although phase-slip events are local, they affect the order parameter throughout the whole sample. Thus, the position and instant in time when the phase slip occurs are determined by the collective dynamics of the order parameter. Consequently, the phase slips cannot be considered independent of each other; therefore, researchers should account for a global trajectory of the order parameter and electric field. This leads to a concept of dynamical state—a well-defined oscillatory trajectory of the order parameter, which consists of one or many phase-slip events per period, with a characteristic period and voltage. Theoretically, the dynamical states are obtained as solutions of the time-dependent Ginzburg-Landau (TDGL) equations (*13*, *14*). A typical solution is periodic in time, with few phase-slip events occurring during one period in different locations along the wire. For a given value of macroscopic parameters (current and temperature), multiple solutions are possible, which correspond to significantly different spatiotemporal trajectories of the order parameter, with a different number of phase slips. By controlling the number of "phase-slip centers" (PSCs) along the wire,

[1]Complex Matter Department, Jozef Stefan Institute, Jamova 39, 1000 Ljubljana, Slovenia. [2]Center of Excellence on Nanoscience and Nanotechnology Nanocenter, Jamova 39, 1000 Ljubljana, Slovenia. [3]Department of Physics, University of Antwerp, Groenenborgerlaan 171, 2020 Antwerp, Belgium. [4]Jozef Stefan International Postgraduate School, Jamova 39, Ljubljana, Slovenia. [5]Department of Physics, Faculty for Mathematics and Physics, University of Ljubljana, Jadranska 19, Ljubljana, Slovenia.
*These authors contributed equally to this work.
†Present address: Institute of Physics, Laboratory for Ultrafast Microscopy and Electron Scattering, École Polytechnique Fédérale de Lausanne (EPFL), Lausanne, Switzerland.
‡Corresponding author. Email: dragan.mihailovic@ijs.si

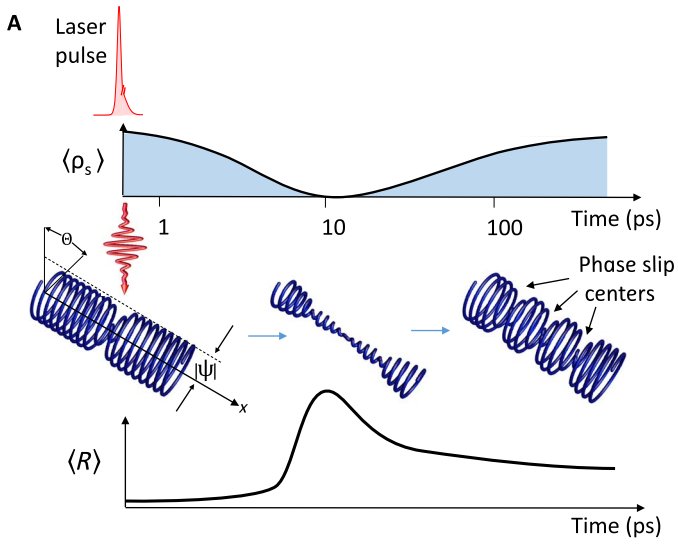

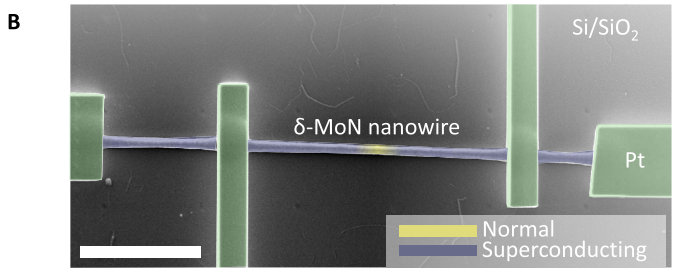

Fig. 1. Schematic representation of the experiment. (**A**) Schematic representation of the evolution of the averaged superfluid density $\langle \rho_s \rangle$, the order parameter $\psi = |\psi| e^{i\Theta}$, and the average resistance $\langle R \rangle$ upon photoswitching between different phase-slip configurations. Absorption of the pulse leads to the transient reduction of the order parameter, eventually resulting in a state with more PSCs and a higher resistance. (**B**) SEM image of the MoN nanowire. Pt contacts are shown in green. Blue and yellow false colors schematically indicate superconducting and normal regions of the sample, representing putative PSCs. White marker length is 5 μm.

one can control the resistance of a wire in a quantized fashion (*15*–*20*), observable as well-defined steps in a current-voltage measurement.

The interest in phase slips has been recently revived, partially due to an increased interest in quantum computations. Quantum PSCs (QPSCs) have been put forward as possible replacements for Josephson junctions in qubits (*21*). Astafiev *et al.* (*22*) demonstrated coherent quantum phase slips in InO_x, whereas Chen *et al.* (*15*) recently showed preservation of the quantum coherence in the presence of the dissipative phase slip in Zn and Al. An observation of QPSCs has stimulated interest in the control of these states. Reversible control of conventional current-driven PSCs with short current pulses was recently demonstrated (*16*). Here, the switching occurred between two different dynamical states, which were formerly observed in cyclic current-voltage measurements.

Here, we present another approach to the control of the phase-slip dynamics: Because the phase-slip process is periodic in time, we can try to manipulate the temporal evolution of the order parameter in nanowires by ultrashort light pulses. We report a successful observation of photoinduced ultrafast transitions between different dynamical states achieved in a δ_3-MoN nanowire. To our knowledge, this is the first observation of an ultrafast transition in dynamical auto-oscillating states in long-range ordered electronic systems. We show that the transition is conceptually different from the current-driven transition. This is manifested in an observation of adiabatically inaccessible long- and short-lived hidden states. The observations are supported by modeling using TDGL equations under nonequilibrium conditions, which gives good insight into the underlying physics without resorting to microscopic theory.

RESULTS

We performed photoexcitation of dynamical states by applying individual 50-fs infrared laser pulses to thin superconducting nanowires under different current bias conditions and temperatures, with the aim of exploring the relevant phase space. Figure 1 shows schematically the photoexcitation process, the time evolution of the superconducting order parameter, and the resistance. The photon energies below and above the Si substrate bandgap (0.95, 1.13, and 1.5 eV) were used to eliminate the possible effects of substrate heating by the laser. A scanning electron microscopy (SEM) image of the circuit is shown in Fig. 1B (more details in Materials and Methods). The experiments were performed on well-characterized δ_3-MoN superconducting nanowires (*16*). δ_3-MoN is a Bardeen-Cooper-Schrieffer superconductor with a relatively high T_c of ≃ 14 K so that the phase-slip dynamics can be studied in a wide range of intermediate temperatures, where neither thermal fluctuations in the vicinity of T_c nor excessive self-heating at low temperatures strongly affects the superconductors' dynamics.

In Fig. 2A, we present a voltage-current (*V*-*I*) map showing the different states that are reached under different conditions. The gray line represents the states that are observed while slowly varying the current *I*, without laser illumination. The colored symbols show the states observed in the laser switching experiment. The data are obtained by exposing the sample to one 50-fs laser pulse every 2 s while measuring the voltage *V* at a constant current. The fluence of the laser pulses is ramped, and when voltage switching occurs, the beam is blocked and the value of the switching fluence is recorded (Fig. 2B).

We label each state that we can unambiguously identify by its voltage *V* drop with an index $|i\rangle$ (i = 0..4, h). Certain states that we address as a single state are actually sets of states with a close value of voltage drops and small steps in the voltage within the set, namely, states $|4\rangle$ and $\langle h|$. We mark the states by two criteria according to their stability and accessibility. Because most states are adiabatically accessible and stable, we use no special notation besides the index $|i\rangle$. Instead, we use the letters "*q*" and "*h*" to mark quasi-stable or hidden states, as explained below. We intentionally introduce the new term "quasi-stable state" and avoid using the term "metastable state," because the latter usually refers to a time-independent stationary state separated from the equilibrium by a potential barrier. For the dynamical states, the energetic properties of the system, for instance, the chemical potential, constantly vary in space and time (*12*) and thus do not directly define the stability of the state. The susceptibility of the order parameter trajectory to thermal and electrical fluctuations is more crucial.

The voltage drop of each state can be ascribed to the dissipation by the normal carriers, accounting for their constantly changing spatially dependent density (*12*). At currents just above the critical value, where each phase slip does not significantly affect the other phase slips, the total differential resistance dV/dI is the sum of the contributions of each PSC $2\Lambda\rho/A$, where Λ is the electric field penetration depth, ρ is the resistivity of the material, and *A* is the cross-sectional area of the wire. We

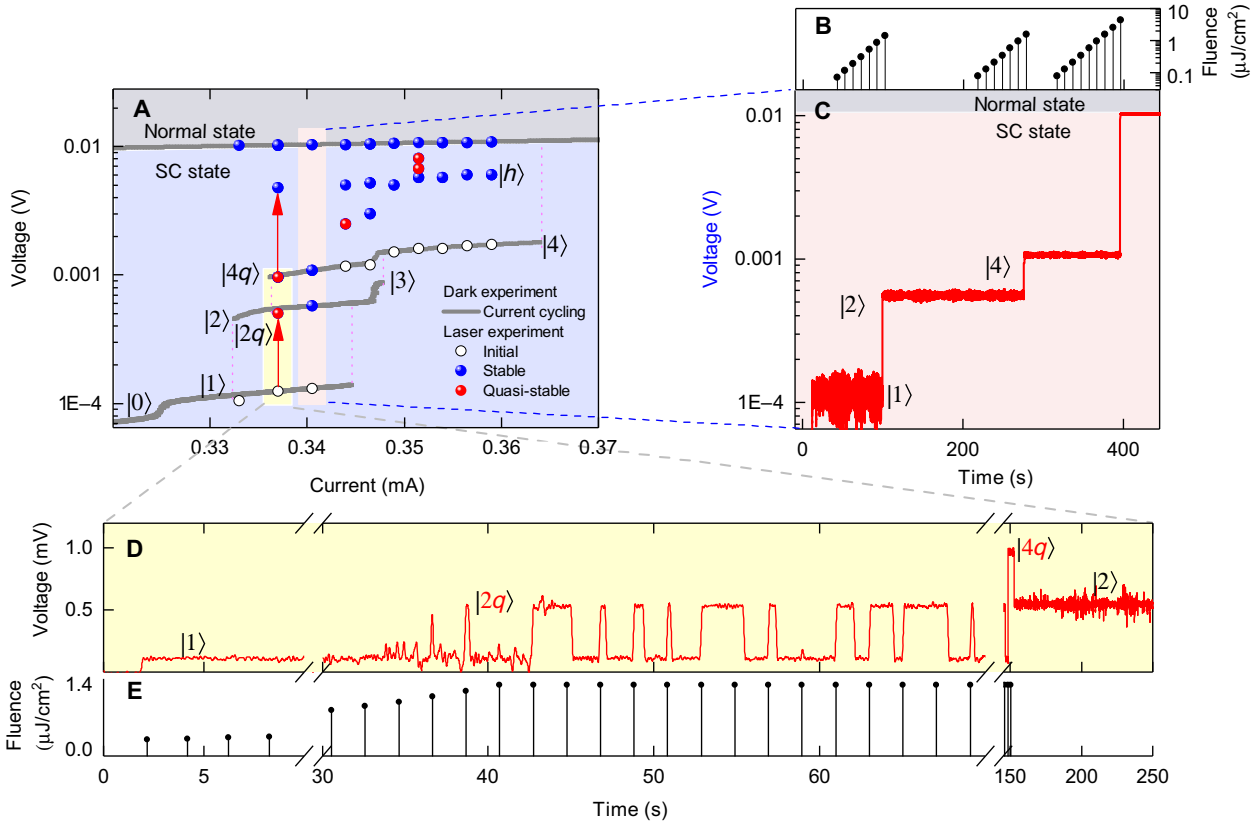

Fig. 2. Optical switching to the stable and quasi-stable states. (**A**) Current-voltage map of accessible dissipative states at 9.2 K. Gray line marks the states that are obtained in current cycling. Spheres show the states observed in the laser switching experiments at fixed values of the current: White, blue, and red symbols represent the initial, stable photoinduced, and quasi-stable photoinduced states, respectively. Note that the numbers do not correspond to the actual number of PSCs. (**B**) Time dependence of the laser fluence, which corresponds to the switching experiment in (C); 1100-nm, 50-fs-long laser pulses arrive every 2 s. (**C**) Switching between stable dynamical states at $i = 0.3405$ mA. (**D**) Example of switching into the quasi-stable state $|2q\rangle$ ($i = 0.337$ mA). For comparison, the later event of spontaneous decay of state $|4q\rangle$ into the stable state $|2\rangle$ obtained in the same experiment is shown. (**E**) Pointers mark the arrival of the laser pulses in the same experiment as in (D); the length of the pointers is proportional to the pulse energy. Switching to state $|2q\rangle$ occurs after nearly every pulse after a threshold pulse energy has been achieved. Experiments in (B) and (C) as well as (D) and (E) are conducted at fixed currents, which are highlighted in (A) by pink and yellow rectangles, respectively.

estimate $\Lambda \sim 43$ nm (*12*, *23*), which gives the number of PSCs to be 5 and 7 for states $|0\rangle$ and $|1\rangle$, respectively. However, for the states with higher voltage drop, the differential resistance becomes significantly nonconstant, indicating strong interactions between phase slips and thus the inapplicability of the abovementioned expression.

Laser control of transitions between known dynamical states

The voltages corresponding to stable or quasi-stable states reached after photoexcitation are shown in Fig. 2A (blue and red symbols). Some of these voltages correspond to the voltages of the states observed in the "dark" experiment (gray line). Let us consider the experiment with current fixed to 0.3405 mA (Fig. 2, A to C, pink rectangle). Upon laser fluence increase, we observe switching from state $|1\rangle \rightarrow$ state $|2\rangle \rightarrow$ state $|4\rangle \rightarrow$ normal state, all of which are stable; that is, they do not decay during the observation time, which is typically longer than 1 min. All of these stable states at any current are marked with blue symbols in Fig. 2A.

Of particular interest are quasi-stable states (red circles on the current-voltage diagram, Fig. 2A) that spontaneously decay on the experimental timescale but have a lifetime significantly longer than our voltmeter time constant of ~1 μs. For example, in Fig. 2D, we observe state $|2q\rangle$ with a lifetime of 0.73 s (note S4). The state is reexcited by nearly every laser pulse until the threshold value of the fluence is reached (Fig. 2E). For a slightly larger fluence, the system switches to state $|4q\rangle$, which then rapidly decays to the stable state $|2\rangle$. The discussed states are highlighted by the yellow rectangle in Fig. 2A.

Hidden states

Thus far, we have discussed the optical switching that occurred between the states that have also been observed in dark experiments, and thus can be reached by applying either a laser pulse or a current pulse (*16*). For current pulses, the transition occurs because the current through the wire exceeds the stability region of the initial state, and dissipations drive the superconductor toward the new, more dissipative stable dynamical state, which remains stable after the pulse is over. However, with laser excitation, we are also able to create new states, implying that the switching mechanism cannot be reduced only to the current increase due to photoinduced carriers. In Fig. 2A, we show numerous stable and quasi-stable states that are not observed in current cycling experiments.

To understand the difference between excitation by current pulses and optical excitation, we investigate the region of stability of such photoexcited hidden states by varying the temperature and the bias

current. We concentrate on the state denoted as $|h\rangle$ in Fig. 2A. This state is stable and is accessible by laser switching over a wide range of currents (Fig. 2A). We first photoexcite the system into the $|h\rangle$ state and then sweep the current in both directions at different temperatures. The resulting plateaus of stability are shown for two temperatures in Fig. 3 (A and B). From Fig. 3A, one can see that at 10 K, which is relatively close to the critical temperature (14 K), the hidden state is also stable at currents higher than in the initial state $|4\rangle$, implying that it can also be accessed by ramping up the current. This was confirmed by subsequent current cycling experiments. However, at lower temperatures (Fig. 3B), this is not the case, and the hidden state becomes unstable at lower bias currents than does the initial state $|4\rangle$.

The regions of stability of the two states ($|4\rangle$ and $|h\rangle$) in the temperature range between 8 and 11 K are summarized in the phase diagram shown in Fig. 3C. The two partially overlap, with their edges crossing at ~9 K. Any adiabatic current or temperature excitation can be represented as a line on this diagram. The necessary condition for the switching to the hidden state is that this line should leave the region of stability of the initial state $|4\rangle$ and enter the region of stability of the final state $|h\rangle$ without crossing the outside region, which would imply a transition into the normal state. The purple dashed line shows an example of this trajectory.

Modeling

Here, we consider the relevant photoinduced processes, estimate their timescales, and then provide a minimal formulation of the TDGL model, which can grasp the physics of the presented phenomenon. This is confirmed by observing the hidden dynamical states in numerical simulations.

The nonequilibrium response of superconductors, such as MoN and NbN, to femtosecond laser pulses is relatively well understood (*24*, *25*). In the strong excitation regime ($P_{switching}$ ~ 150 mJ/cm^3), the superconducting condensate is suppressed by pair-breaking and quasi-particle excitation by phonons emitted in the photoexcited carrier thermalization process, which occurs within one optical penetration depth (λ_{op} = 17 nm) on the surface of the nanowire within a time τ_{sup} of ~1 to 3 ps. Our calculations suggest that the lattice is also heated above T_c, thus creating a highly nonhomogeneous distribution of quasi-particle temperature and superfluid density (see note S1 for detailed thermal analysis). Further dynamics is defined by heat diffusion into the bulk of the nanowire and heat exchange with the He exchange gas in the cryostat. The former can be estimated and results in surface cooling on a timescale of hundreds of picoseconds. This is on the same timescale as the directly measured phonon escape time for NbN thin films (*24*, *25*). Thus, the role of the laser pulse is to transiently suppress the order parameter, resetting the phase and allowing the highly dissipative state to be rapidly stabilized. This occurs on a timescale that is much faster than the time between phase-slip events τ_{ps}, which is usually in the gigahertz range (*23*, *26*).

We proceed by looking for a minimal theoretical model to describe optical switching and hidden states. There were two main directions in theoretical developments of phase-slip phenomenon: (i) phenomenological theories that aim for a precise description of *I*-*V* characteristics of a single phase slip, in which the phase-slip event is usually grafted through the assumptions (*12*, *27*, *28*), and (ii) dynamical theories of superconductivity; namely, various formulations of the TDGL model in which phase slips naturally appear as solutions of nonlinear equations (*13*, *14*, *29*) [see the study of Tidecks (*14*) for a detailed overview]. The first set of theories is not suitable for our experiments, because these theories do not provide the details of multiple phase-slip processes and consider each phase slip as an independent event. The numerical solution of the TDGL model can instead realistically describe current-voltage characteristics of superconducting nanowires and provide the realization of a multistability phenomenon (*30*, *31*).

In the following, we present the simulations of the effect of the short laser pulse on the phase-slip behavior within the usual 1D-TDGL model. This formulation does not account for the nonthermal distribution of quasi-particles and omits explicit inclusion of the superconducting gap. Still, it has been shown that the description of the

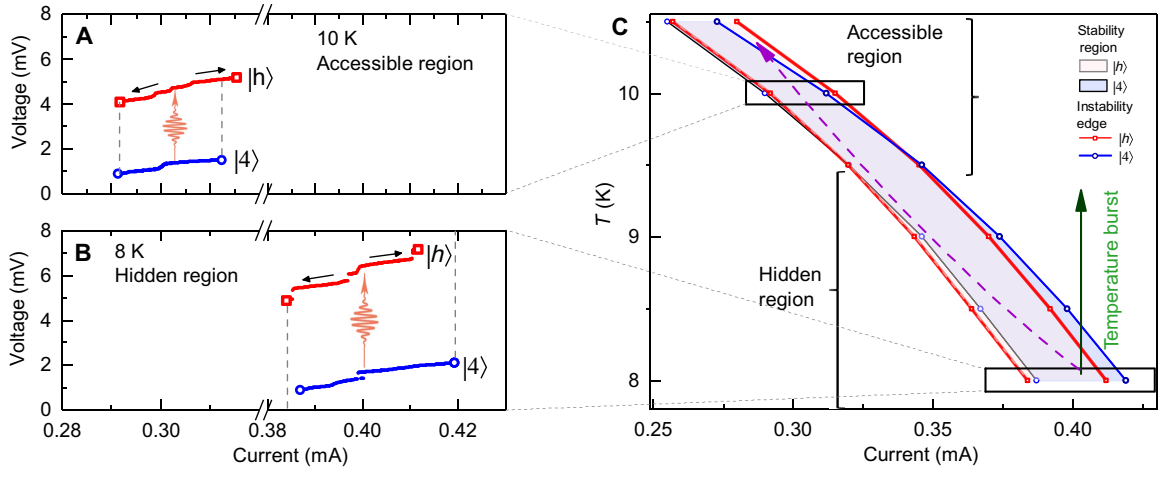

Fig. 3. Analysis of the accessibility of the hidden state. (**A** and **B**) Current cycling after photoexcitation of the hidden state at high and low temperatures, respectively (red lines). Current cycling of the initial state $|4\rangle$ is shown by blue solid lines. Edge points at which the transition occurs are marked by open symbols. In (A), the $|h\rangle$ state is accessible with both current and optical stimulus. In (B), the $|h\rangle$ state does not exist at the high-current edge point of state $|4\rangle$ and thus can only be accessed by photoexcitation. (**C**) Current-temperature map of the stability regions of the $|h\rangle$ and $|4\rangle$ states from experiments in (A) and (B) at a number of temperatures. The high-current instability edges of the $|h\rangle$ and $|4\rangle$ states are shown in red and blue solid lines, respectively. The $|h\rangle$ state is accessible through the instability if the transition occurs above 9.5 K, where the instability line of the initial state (blue) falls into the stability region of the $|h\rangle$ state. The green arrow indicates the trajectory in the case of a temperature surge caused by the laser pulse. The dashed purple line indicates the trajectory required to achieve switching by adiabatic excitation from the same initial state.

phase-slip phenomenon is qualitatively the same as in the more complete generalized TDGL models (*13*, *30*, *32*). We can write the equations, which account for the single-pulse laser excitation, as follows

$$u\left(\frac{\partial\psi}{\partial t}+i\Phi\psi\right)=\alpha(t)\psi-\psi|\psi|^2+\frac{\partial^2\psi}{\partial x^2}$$

$$j_{\text{total}}=-\frac{\partial\Phi}{\partial x}-\frac{\mathrm{i}}{2}\left(\psi^*\frac{\partial\psi}{\partial x}-\psi\frac{\partial\psi^*}{\partial x}\right) \quad (1)$$

Here, $\psi=|\psi|e^{i\theta}$ is the complex order parameter, where θ is the phase of the order parameter, j_{total} is the total current through the wire, Φ is the electrostatic potential, and u is a material-dependent parameter defined as the ratio of the amplitude and phase relaxation times. Time and length are measured in units of the amplitude relaxation time ($\tau_{GL}\approx\frac{0.7\hbar}{\Delta}\left(1-\frac{T}{T_c}\right)^{-1}\sim 2\text{ps}$) (*33*) and the coherence length (ξ ~ 6.5 nm). The photoexcitation is modeled by the time-dependent reduced electronic temperature $T/T_c=1-\alpha(t)=P[1-0.5\,\text{erfc}\left(\frac{t}{\tau_{sup}}\right)]e^{-t/\tau_{rec}}/\tau_{rec}$, where the peak reduced temperature P is proportional to the square root of the laser pulse energy, and erfc is the complementary error function.

In Fig. 4A, we plot the solution of Eq. 1, which demonstrates switching into a hidden state, caused by an ultrafast temperature pulse ($\tau_{rec}=0.01\tau_{ps}$). Before the laser pulse arrives, the system is characterized by two phase slips per period (Fig. 4A, left) and a time-average voltage drop across the wire $\langle V_i\rangle=0.071\hbar/(2e\tau_\theta)$ (Fig. 4B). The period of the periodic process is ~ 352 τ_{GL}. It is important to highlight the crucial role of parameter u and the length of the wire in the creation of PSC (*31*). If $u>1$, that is, the phase of the order parameter relaxes faster than its amplitude, then each consecutive phase slip appears at the same spot at the center of the wire. The solutions with $u<1$ are more realistic and correspond to spatially inhomogeneous phase slips. The longer the wire, the more inequivalent solutions can be obtained. We found that setting $L=40\xi$ is sufficient to qualitatively reproduce the phenomenon of the laser switching.

The laser pulse results in a strong transient suppression of the order parameter. From this transient state, the system evolves toward a solution with three phase slips per period and a larger voltage drop $\langle V_h\rangle=0.08\hbar/(2e\tau_\theta)$ (Fig. 4, A and B). This state appears to be stable on the entire timescale of the simulation of $5\times10^4\tau_{GL}$ (note that in Fig. 4A, we have shown only the first $3\times10^3\tau_{GL}$ at the beginning of the simulation).

The calculations show that one cannot reach this state by gradual variation of the current. We also show that this new state is hidden; that is, it is stable only with a fast temperature quench. With slow cooling ($\tau_{rec}=20\tau_{ps}$), the $|h\rangle$ state is transient and decays before the system cools to its initial temperature (note S2).

We remark that the comparison of the simulations and the experiment is only qualitative. The length of the nanowire used in the computation is 40ξ, which is sufficient to produce a decent number of non-identical dynamical states but is drastically smaller than the realistic value of ~1600ξ. Parameter u was set to 0.5 in accordance with our previous study (*16*, *30*, *31*). Although it is larger than experimentally estimated $=\left(\frac{\xi}{\Lambda}\right)^2\sim0.023$, both values describe the same regime of hysteretic current-voltage characteristics (*31*), thus giving a qualitatively similar description. Most crucially, the ratio of the temperature relaxation time and the phase-slip period is estimated from the experiment as described above. Both of these values are much larger than the amplitude relaxation time τ_{GL}. We note that the actual optical pulse duration is not important because the dynamics is defined by lattice rather than electron temperature evolution. Finally, this model ignores Joule heating by the laser pulse and dissipation by the PSC fluctuations, which do not qualitatively change the periodic behavior of the order parameter (*12*, *15*, *25*).

DISCUSSION

The presented modeling shows that dynamical stabilization of the transient states can be set up within a TDGL model with very few assumptions, which means that the phenomenon is universal. We can see that the dynamical behavior of the superconductor changes in a discrete fashion through optically induced transitions and that the switching requires a strong suppression of the condensate. This implies that each time an optical pulse arrives, it acts as a trigger for the PSC oscillations, resetting the phase of the oscillation. This mechanism is most likely responsible for the transition not only into the hidden states but also between the visible states (Fig. 2C).

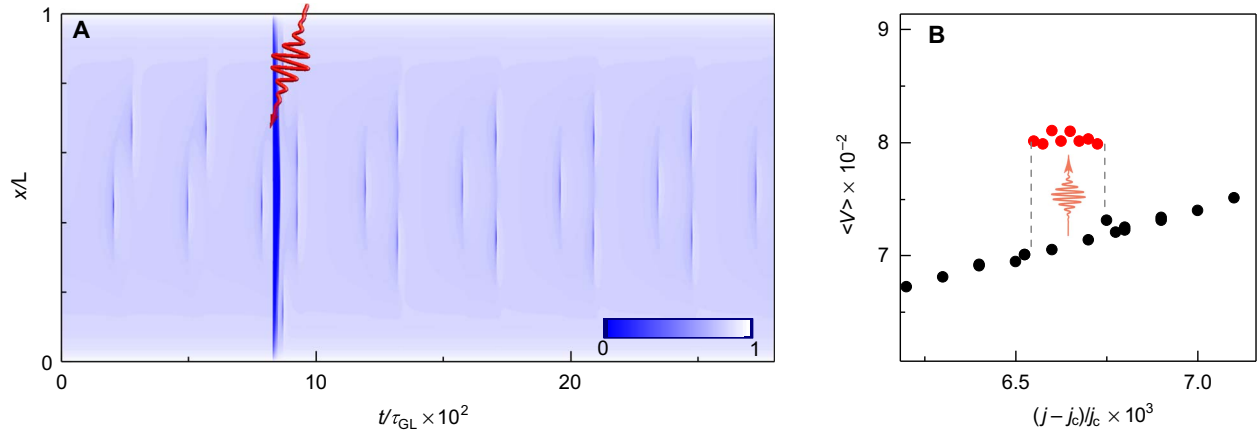

Fig. 4. Predicted real-time dynamics of the order parameter through a photoinduced transition to a hidden dynamically stable state. (**A**) The order parameter amplitude $|\psi|$ is plotted as a function of time and coordinate along the nanowire. The timing of the laser pulse is indicated. (**B**) Average voltage $\langle V\rangle$ as the current is ramped up and down in both states to test stability, similar to the experiments in Fig. 3. Voltage is calculated in units of $\hbar/(2e\tau_\theta)$.

In the presented simulations, the two considered states produced significantly different voltages across the nanowire. However, similar simulations show that different dynamical states can also have similar values of voltage drop but belong to different limit cycles (*30*). The photoinduced short-lived state $|2q\rangle$ and the stable state $|2\rangle$ achievable by optical and current excitations in the experiment are examples of such a situation (Fig. 2D). These states are characterized by similar values of the voltage drop of 0.53 ± 0.012 mV and 0.55 ± 0.046 mV, respectively; however, the fact that they have different lifetimes and voltage noise amplitude (Fig. 2D) and that they are reached by different routes in parameter space suggest that the two states are different in nature; that is, they correspond to different trajectories of the order parameter. We emphasize that because of their short-lived nature, quasi-stable states are, in principle, unobservable under gradual variation of the current and temperature.

Thus far, we have not discussed the possibility that transitions to hidden states are caused by slow quasi-adiabatic laser heating and an associated current increase. These two effects would correspond to upward vertical and rightward horizontal trajectories, respectively, in the current temperature plane of the phase diagram in Fig. 3C, and their sum would result in the upright directed trajectory (for example, a temperature surge is shown by the green arrow in Fig. 3C). However, none of these possibilities can lead to the transition from state $|4\rangle$ to state $|h\rangle$ as long as the initial temperature is $T < 9.5$ K and $j > 0.34$ mA; instead, the normal state will be reached. We denote this area in Fig. 3C as the hidden region of the phase diagram. At higher temperatures and lower currents, we see that the two states behave in a more usual way; that is, the more dissipative state survives up to higher currents. In this case, transition is possible as a result of both current and temperature pulses. This part of the current-temperature diagram in Fig. 3C is marked as the accessible region.

No matter what the initial current and temperature are, the transition between the two states with adiabatic, near-equilibrium perturbation is possible only through the accessible region. In contrast, if the initial state of our system is in the hidden region, then this scenario would imply laser cooling and current reduction, which is unphysical. We conclude that nonequilibrium perturbation by the laser cannot be replaced by any kind of adiabatic perturbation. The implication is that some of the dynamically stable states can be reached only by nonequilibrium suppression of the superfluid density caused by short pulses, underlining their hidden nature.

Theoretical simulations provide an insight into the formation of the hidden state. In Fig. 4A, the recovery of the order parameter after the laser pulse occurs on a timescale comparable to the recovery after the phase slip. Moreover, we notice that photoinduced phase slips are more evenly distributed along the wire than initially. This reflects the homogeneous suppression of the order parameter by the laser pulse. We can assume that a large number of evenly distributed phase slips are a general feature of photoinduced states. This can explain why we do not observe any photoswitching at lower currents; this is because there are no stable trajectories with many phase slips.

We can conclude that the observed laser switching results from highly controllable dynamical stabilization of quantized current states, observed for the first time in a dynamical long-range ordered quasi-1D condensed matter system. The switching is controllable with high precision, determined by the laser timing. Which dynamical states are reached at a given temperature is primarily controlled by the bias current and laser pulse fluence. The dynamical stabilization can be presented graphically within the TDGL model. Improved modeling of the experiment may be performed by including the effects of dissipation and quasi-particle dynamics, which are ignored in our toy model. The character of the transition implies a precise control of timing (that is, phase) of PSC oscillations and their number, which opens the way to nanoscale ultrafast optoelectronic devices operating with very small switching voltages in the millivolts range and at very high frequencies (10 to 1000 GHz, only limited by thermal relaxation properties). Fundamentally, this is the first experimental realization of hidden dynamical states in a quantum system. The nonequilibrium nature of the transition to the hidden state is evident from the current-temperature phase diagram analysis and theoretical simulations, and represents an important step toward a vast uncharted territory of nonequilibrium phase diagrams in condensed matter systems.

MATERIALS AND METHODS

Nanowire material preparation

δ_3-MoN (highly ordered hexagonal phase of MoN) nanowires were produced by transformation from $Mo_6S_yI_z$ nanowires (*34*) with diameters between 13 and 320 nm. The $Mo_6S_yI_z$ nanowires used as templates were prepared from the elements in a single-zone furnace at T = 1040°C (*35*), where y and z refer to the initial stoichiometry in the synthesis, within the range of $8.2 < y + z < 10$. The transformation of MoSI nanowires into δ_3-MoN nanowires was carried out inside a tube furnace with a constant flow of argon and ammonia at T = 825°C (*36*).

Electrical measurements

Wires with different diameters were dispersed in an ultrasonic bath in acetonitrile for 5 min at 80 kHz and centrifuged at 385*g* to remove heavy agglomerates by sedimentation. The remaining dispersion was spray-casted on a silica substrate and examined under SEM. Focused ion beam (FIB)–induced platinum deposition was made using beams with 30-kV acceleration voltage and current of 80 to 430 pA with an FEI Helios NanoLab 650 instrument. The thickness of the deposition were roughly 1 μm. The resistance measurements were done with the four-contact method using a Keithley 6221/Keithley 2182A setup. All the measurements were conducted in the constant current mode.

Laser source

Ti:sapphire regenerative amplifier (50 fs, 1 kHz) was used as a pulse source. Laser wavelength was subsequently varied with an optical parametric amplifier. One pulse per 2 s was transmitted from the pulse train with a homemade mechanical shutter. The laser beam was focused on an 80-μm-diameter spot. Laser fluence was controlled with a motorized variable optical density wheel.

To eliminate the substrate heating as a possible origin of the switching, we compared the switching threshold fluence under and above the absorption edge of silicon at 1300 and 1100 nm, respectively. Both sets of values were identical within the experimental error of 20%.

SUPPLEMENTARY MATERIALS

Supplementary material for this article is available at http://advances.sciencemag.org/cgi/content/full/4/3/eaao0043/DC1

note S1. Calculation of the initial electronic temperature evolution.

note S2. TDGL modeling. Case of quasi-equilibrium cooling.

note S3. Phase trajectories of the order parameter in the initial and hidden states. Role of the synchronization between laser pulses and the phase-slip process.

note S4. Decay of the quasi-stable state.

fig. S1. Estimated electronic temperature evolution across the nanowire.
fig. S2. Spatiotemporal evolution of the order parameter amplitude in the case of the quasi-equilibrium cooling (time is horizontal and changes continuously from left to right, from top to bottom).
fig. S3. Cut of the phase trajectory of the order parameter at the center of the nanowire in the $|\psi|$ – E (order parameter amplitude – electric field) phase space.
fig S4. Distribution of the lifetimes of the quasi-stable state $|2q\rangle$.
References (*37*–*39*)

REFERENCES AND NOTES

1. M. S. Turner, F. Wilczek, Is our vacuum metastable? *Nature* **298**, 633–634 (1982).
2. K. Nasu, *Photoinduced Phase Transitions* (World Scientific Publishing, 2004).
3. V. R. Morrison, R. P. Chatelain, K. L. Tiwari, A. Hendaoui, A. Bruhács, M. Chaker, B. J. Siwick, A photoinduced metal-like phase of monoclinic VO_2 revealed by ultrafast electron diffraction. *Science* **346**, 445–448 (2014).
4. D. Fausti, R. I. Tobey, N. Dean, S. Kaiser, A. Dienst, M. C. Hoffmann, S. Pyon, T. Takayama, H. Takagi, A. Cavalleri, Light-induced superconductivity in a stripe-ordered cuprate. *Science* **331**, 189–191 (2011).
5. A. Kirilyuk, A. V. Kimel, T. Rasing, Ultrafast optical manipulation of magnetic order. *Rev. Mod. Phys.* **82**, 2731–2784 (2010).
6. L. Stojchevska, I. Vaskivskyi, T. Mertelj, P. Kusar, D. Svetin, S. Brazovskii, D. Mihailovic, Ultrafast switching to a stable hidden quantum state in an electronic crystal. *Science* **344**, 177–180 (2014).
7. H. Ichikawa, S. Nozawa, T. Sato, A. Tomita, K. Ichiyanagi, M. Chollet, L. Guerin, N. Dean, A. Cavalleri, S.-i. Adachi, T.-h. Arima, H. Sawa, Y. Ogimoto, M. Nakamura, R. Tamaki, K. Miyano, S.-y. Koshihara, Transient photoinduced 'hidden' phase in a manganite. *Nat. Mater.* **10**, 101–105 (2011).
8. W. H. Zurek, Cosmological experiments in condensed matter systems. *Phys. Rep.* **276**, 177–221 (1996).
9. S. Koshihara, Y. Tokura, T. Mitani, G. Saito, T. Koda, Photoinduced valence instability in the organic molecular compound tetrathiafulvalene-*p*-chloranil (TTF-CA). *Phys. Rev. B. Condens. Matter* **42**, 6853–6856 (1990).
10. C. Giannetti, M. Capone, D. Fausti, M. Fabrizio, F. Parmigiani, D. Mihailovic, Ultrafast optical spectroscopy of strongly correlated materials and high-temperature superconductors: A non-equilibrium approach. *Adv. Phys.* **65**, 58–238 (2016).
11. D. Golubchik, E. Polturak, G. Koren, Evidence for long-range correlations within arrays of spontaneously created magnetic vortices in a Nb thin-film superconductor. *Phys. Rev. Lett.* **104**, 247002 (2010).
12. W. J. Skocpol, M. R. Beasley, M. Tinkham, Phase-slip centers and nonequilibrium processes in superconducting tin microbridges. *J. Low Temp. Phys.* **16**, 145–167 (1974).
13. B. I. Ivlev, N. B. Kopnin, Electric currents and resistive states in thin superconductors. *Adv. Phys.* **33**, 47–114 (1984).
14. R. Tidecks, *Current-Induced Nonequilibrium Phenomena in Quasi-One-Dimensional Superconductors*, vol. 121 of *Springer Tracts in Modern Physics* (Springer, 1990).
15. Y. Chen, Y.-H. Lin, S. D. Snyder, A. M. Goldman, A. Kamenev, Dissipative superconducting state of non-equilibrium nanowires. *Nat. Phys.* **10**, 567–571 (2014).
16. J. Buh, V. Kabanov, V. Baranov, A. Mrzel, A. Kovič, D. Mihailovic, Control of switching between metastable superconducting states in δ-MoN nanowires. *Nat. Commun.* **6**, 10250 (2015).
17. W. A. Little, Decay of persistent currents in small superconductors. *Phys. Rev.* **156**, 396–403 (1967).
18. J. S. Langer, V. Ambegaokar, Intrinsic resistive transition in narrow superconducting channels. *Phys. Rev.* **164**, 498–510 (1967).
19. D. E. McCumber, B. I. Halperin, Time scale of intrinsic resistive fluctuations in thin superconducting wires. *Phys. Rev. B* **1**, 1054–1070 (1970).
20. K. Y. Arutyunov, D. S. Golubev, A. D. Zaikin, Superconductivity in one dimension. *Phys. Rep.* **464**, 1–70 (2008).
21. J. E. Mooij, Y. V. Nazarov, Superconducting nanowires as quantum phase-slip junctions. *Nat. Phys.* **2**, 169–172 (2006).
22. O. V. Astafiev, L. B. Ioffe, S. Kafanov, Y. A. Pashkin, K. Y. Arutyunov, D. Shahar, O. Cohen, J. S. Tsai, Coherent quantum phase slip. *Nature* **484**, 355–358 (2012).
23. V. I. Kuznetsov, V. A. Tulin, Synchronization of high-frequency vibrations of slipping phase centers in a tin whisker under microwave radiation. *J. Exp. Theor. Phys.* **86**, 745–750 (1998).
24. K. S. Il'in, M. Lindgren, M. Currie, A. D. Semenov, G. N. Gol'tsman, R. Sobolewski, S. I. Cherednichenko, E. M. Gershenzon, Picosecond hot-electron energy relaxation in NbN superconducting photodetectors. *Appl. Phys. Lett.* **76**, 2752–2754 (2000).
25. M. Beck, M. Klammer, S. Lang, P. Leiderer, V. V. Kabanov, G. N. Gol'tsman, J. Demsar, Energy-gap dynamics of superconducting NbN thin films studied by time-resolved terahertz spectroscopy. *Phys. Rev. Lett.* **107**, 177007 (2011).
26. A. G. Sivakov, A. M. Glukhov, A. N. Omelyanchouk, Y. Koval, P. Müller, A. V. Ustinov, Josephson behavior of phase-slip lines in wide superconducting strips. *Phys. Rev. Lett.* **91**, 267001 (2003).
27. T. J. Rieger, D. J. Scalapino, Time-dependent superconductivity and quantum dissipation. *Phys. Rev. B* **6**, 1734–1743 (1972).
28. A. M. Kadin, L. N. Smith, W. J. Skocpol, Charge imbalance waves and nonequilibrium dynamics near a superconducting phase-slip center. *J. Low Temp. Phys.* **38**, 497–534 (1980).
29. L. Kramer, R. J. Watts-Tobin, Theory of dissipative current-carrying states in superconducting filaments. *Phys. Rev. Lett.* **40**, 1041–1044 (1978).
30. V. V. Baranov, A. G. Balanov, V. V. Kabanov, Current-voltage characteristic of narrow superconducting wires: Bifurcation phenomena. *Phys. Rev. B* **84**, 94527 (2011).
31. V. V. Baranov, A. G. Balanov, V. V. Kabanov, Dynamics of resistive state in thin superconducting channels. *Phys. Rev. B* **87**, 174516 (2013).
32. R. J. Watts-Tobin, Y. Krähenbühl, L. Kramer, Nonequilibrium theory of dirty, current-carrying superconductors: Phase-slip oscillators in narrow filaments near T_c. *J. Low Temp. Phys.* **42**, 459–501 (1981).
33. A. Schmid, A time dependent Ginzburg-Landau equation and its application to the problem of resistivity in the mixed state. *Phys. Kondens. Mater.* **5**, 302–317 (1966).
34. D. Mihailovic, Inorganic molecular wires: Physical and functional properties of transition metal chalco-halide polymers. *Prog. Mater. Sci.* **54**, 309–350 (2009).
35. M. Remškar, A. Mrzel, M. Viršek, A. Jesih, Inorganic nanotubes as nanoreactors: The first MoS_2 nanopods. *Adv. Mater.* **19**, 4276–4278 (2007).
36. J. Buh, A. Kovič, A. Mrzel, Z. Jagličić, A. Jesih, D. Mihailovic, Template synthesis of single-phase δ_3-MoN superconducting nanowires. *Nanotechnology* **25**, 025601 (2014).
37. Yu. P. Gousev, G. N. Gol'tsman, A. D. Semenov, E. M. Gershenzon, R. S. Nebosis, M. A. Heusinger, K. F. Renk, Broadband ultrafast superconducting NbN detector for electromagnetic radiation. *J. Appl. Phys.* **75**, 3695–3697 (1994).
38. S. D. Brorson, A. Kazeroonian, J. S. Moodera, D. W. Face, T. K. Cheng, E. P. Ippen, M. S. Dresselhaus, G. Dresselhaus, Femtosecond room-temperature measurement of the electron-phonon coupling constant γ in metallic superconductors. *Phys. Rev. Lett.* **64**, 2172–2175 (1990).
39. K. Weiser, U. Strom, S. A. Wolf, D. U. Gubser, Use of granular NbN as a superconducting bolometer. *J. Appl. Phys.* **52**, 4888–4889 (1981).

Acknowledgments: We acknowledge T. Mertelj for useful discussions and M. Rigler for ellipsometry measurements. **Funding:** The funding was provided by European Research Council advanced grant TRAJECTORY. **Author contributions:** D.M. came up with the original idea. I.M. and J.B. conducted the experiment and analyzed the data. A.M. synthesized the nanowires. J.B. did FIB fabrication. J.B. and I.M. set up electrical and optical experiments, respectively. V.V.K., V.V.B., and I.M. conducted theoretical calculations. J.B., I.M., and D.M. wrote the manuscript. **Competing interests:** The authors declare that they have no competing interests. **Data and materials availability:** All data needed to evaluate the conclusions in the paper are present in the paper and/or the Supplementary Materials. Additional data related to this paper may be requested from the authors.

Submitted 5 June 2017
Accepted 13 February 2018
Published 30 March 2018
10.1126/sciadv.aao0043

Citation: I. Madan, J. Buh, V. V. Baranov, V. V. Kabanov, A. Mrzel, D. Mihailovic, Nonequilibrium optical control of dynamical states in superconducting nanowire circuits. *Sci. Adv.* **4**, eaao0043 (2018).

Nonequilibrium optical control of dynamical states in superconducting nanowire circuits

Ivan Madan, Joze Buh, Vladimir V. Baranov, Viktor V. Kabanov, Ales Mrzel and Dragan Mihailovic

Sci Adv **4** (3), eaao0043.
DOI: 10.1126/sciadv.aao0043